

# Characterization of titania silicalites

Goutam Deo, Andrzej M. Turek\* and Israel E. Wachs

Zettlemoyer Center for Surface Studies, Department of Chemical Engineering, Lehigh University, Bethlehem, PA, USA

Diana R.C. Huybrechts and P.A. Jacobs

Laboratorium voor Oppervlaktechemie, Katholieke Universiteit, Leuven (Heverlee), Belgium

Titanium-substituted silicalites, prepared from two different silicalite precursors, are characterized using Raman spectroscopy, X-ray absorption spectroscopy, pyridine adsorption, and methanol oxidation. The silicalite precursors used are tetraethyl orthosilicate and Ludox AS 40. Two different types of titania species are observed in the titania silicalites. Below 1.6 mole% Ti/(Ti + Si), a dispersed  $\text{TiO}_x$  species is present that does not possess a terminal Ti=O bond or Brønsted acidity. The (average) structure of the  $\text{TiO}_x$  species changes with the titania substitution into the silicalites, but this structural change, apparently, does not affect the reactivity of the catalytic active center during reactions involving liquid water. This  $\text{TiO}_x$  species in silicalites is active toward redox reactions, and its reactivity is similar to the titania species present on the surface of amorphous  $\text{SiO}_2$  (Cab-O-Sil). Above 1.6 mole% Ti/(Ti + Si),  $\text{TiO}_2$  (anatase) particles are present in addition to the dispersed  $\text{TiO}_x$  species. The  $\text{TiO}_2$  (anatase) particles are not effective in redox reactions and form weak Lewis acid sites. The titania silicalites produced from the different precursors were structurally similar, but differed chemically due to acidic impurities present in Ludox AS 40. The critical factor in determining the reactivities of Ti silicalite and surface titania supported on amorphous silica is the stability of the Ti–O–Si bond in the presence of liquid water.

**Keywords:** Silicalite; titania; silica; Raman; X-ray absorption; methanol oxidation; pyridine adsorption

## INTRODUCTION

Titanium-substituted silicalites (TS-1)<sup>1</sup> exhibit exceptional catalytic activity and selectivity for mild oxidation reactions.<sup>2–4</sup> Transition-metal complexes, using a mild oxidant, are able to hydroxylate alkanes but the selectivities are usually unsatisfactory.<sup>3–4</sup> Titanium silicalites, on the other hand, are able to selectively convert alkanes, as well as alkenes, aromatics, and alcohols.<sup>2–5</sup> These interesting properties of the titanium silicalites raises the question of the nature of the titanium sites that are present in such materials.

Previous characterization studies of the titania silicalites were sketchy and usually did not provide a detailed analysis of the active titanium phase. X-ray diffraction (XRD) techniques were used to study the changes in cell parameters of the various titanium-substituted silicalites. From the changes in cell parameters, a tetrahedral coordination of the titanium oxide species was proposed.<sup>5</sup> Infrared (i.r.) spectroscopic studies indicated a band at  $960\text{ cm}^{-1}$ , which

increases with titanium substitution.<sup>1</sup> This  $960\text{ cm}^{-1}$  band was attributed to the Ti=O vibration<sup>3,5</sup> or the  $\text{SiO}_4\text{---Ti}$  vibrations<sup>6</sup> and was observed to slightly change upon addition of moisture (shifts the band to  $\sim 975\text{ cm}^{-1}$  with intensity weakening and broadening), methanol (broadening and weakening), and ammonia (broadening and weakening).<sup>6</sup> All these changes were reversible in nature. A five-coordinated titania structure was also proposed based on the ultraviolet visible (u.v.-vis) spectrum of  $\sim 1.0$  mole% Ti/(Ti + Si) silicalite that possessed a transition at  $48,000\text{ cm}^{-1}$  and was assigned to a hydroxylated titania structure.<sup>6</sup> Fast atom bombardment mass spectroscopy (FABMS)<sup>7</sup> and electron diffraction X-ray (EDX) analysis<sup>5</sup> indicated that the titanium was well dispersed in the silicalite. The  $^{29}\text{Si}$  magic angle spinning nuclear magnetic resonance (MAS n.m.r.) investigations indicate that the silicalite matrix is affected by the substitution of titania, as the multiplet characteristics of the silicalites broadens and a shoulder appears in the high-field region of the signal.<sup>5</sup> Using electron paramagnetic resonance (e.p.r.) spectroscopy, it was concluded that tetravalent titanium present in the titania silicalites is reduced to a trivalent titanium in tetragonally distorted octahedral symmetry.<sup>8</sup> X-ray absorption studies (XANES) of a single, unspecified titanium-substituted silicalite sam-

\* On leave from Faculty of Chemistry, Jagiellonian University, Cracow, Poland.

Address reprint requests to Dr. Wachs at the Zettlemoyer Center for Surface Studies, Department of Chemical Engineering, Lehigh University, Bethlehem, PA 18015, USA.

Received 10 June 1991; accepted 14 November 1991

ple concluded that the titania is present in different coordinations (four, five, and six) and the amount of octahedral titania decreases upon dehydration.<sup>9</sup>

Recent characterization studies of Huybrechts et al. used i.r. and u.v.-vis techniques on various titanium-substituted silicalite catalysts.<sup>10</sup> The silicalites were obtained from two sources: tetraethyl orthosilicate and Ludox. The amount of titanium that was effectively substituted depended on the specific preparation of the silicalite (from tetraethyl orthosilicate or commercial Ludox). A better substitution was observed with the silicalite prepared from tetraethyl orthosilicate. It was observed that the  $960\text{ cm}^{-1}$  band in the i.r. increases with titanium substitution and then levels off. U.v.-vis results of the titania silicalites show an absorption at wavenumbers higher than  $34,000\text{ cm}^{-1}$  for the initial titanium-substituted samples, and for higher substitutions, an absorption at  $30,800\text{ cm}^{-1}$  is observed, characteristic of  $\text{TiO}_2$  (anatase) particles. The detection of  $\text{TiO}_2$  (anatase) particles for higher substitutions correlates well with the leveling off of the  $960\text{ cm}^{-1}$  i.r. band and the catalytic properties of the titania silicalites. In addition, hydroxyl vibrations in the i.r. spectra arising from the substituted titania species were not observed, contrary to the hydroxylated structure proposed by Boccuti et al.,<sup>6</sup> which should give rise to additional hydroxyl vibrations.

In the present study, we used Raman spectroscopy, pyridine adsorption, X-ray absorption near edge spectroscopy (XANES), and the methanol oxidation reaction as the characterization tools for determining the nature of the titanium oxide species present in the titania silicalites. The combined analysis of the various physical and chemical characterization techniques provides further insight into the fundamental understanding of the titanium oxide species in titania silicalites and its reactivity. In addition, the structure and reactivity of the molecularly dispersed titania species on amorphous silica surfaces ( $\text{TiO}_x/\text{SiO}_2$ ) was studied to outline the similarity and differences between the titania silicalites and  $\text{TiO}_x/\text{SiO}_2$ .

## EXPERIMENTAL

### Sample preparation

#### *Ti silicalites*

The Ti silicalite samples were made by hydrothermally treating a mixture of (1) tetraethyl orthotitanate (Aldrich), tetraethyl orthosilicate, referred to as TSEx1 samples from here on, or Ludox AS 40 (ammonium stabilized 40% silica sol [DuPont], referred to as TSEx2 samples from here on; (2) an organic template (tetrapropylammonium hydroxide); and (3) water, according to Perego et al.<sup>5</sup> XRD patterns of the Ti silicalite show the presence of the pentasil-type framework structure. Chemical analysis was done by ICP analysis after fusion of the sample using alkali carbonate or  $\text{HF-H}_2\text{SO}_4$ . The nomenclature of the Ti silicalite samples are identical to those of the previous study by Huybrechts et al.<sup>10</sup>

#### *2% $\text{TiO}_2$ supported on $\text{SiO}_2$*

Molecularly dispersed titania was prepared on  $\text{SiO}_2$  (Cab-O-Sil,  $300\text{ m}^2/\text{g}$ ) by the incipient wetness impregnation of a nonaqueous solution of  $\text{Ti}[\text{OCH}(\text{CH}_3)_2]_4$ . The appropriate amount of the titania precursor, corresponding to 2%  $\text{TiO}_2$  by weight, was dissolved in a known volume of toluene. Due to the moisture sensitive nature of the titania precursor, the titania precursor-toluene solution, impregnation, and drying (room temperature for 16 h and  $110^\circ\text{C}$  for 16 h) were all carried out under a nitrogen atmosphere. Final calcination of the samples were carried out in oxygen for 16 h. This sample is referred to as 2%  $\text{TiO}_2/\text{SiO}_2$ . The Raman spectrum of the 2%  $\text{TiO}_2/\text{SiO}_2$  sample indicates that the titanium oxide surface species was molecularly dispersed and that  $\text{TiO}_2$  crystalline phases were absent.

### Raman spectroscopy

Laser Raman spectra were obtained with an  $\text{Ar}^+$  laser tuned at  $514.5\text{ nm}$  and delivering 1–100 mW of power at the sample. The scattered radiation from the sample was directed into an optical multichannel analyzer equipped with a photodiode array. The Raman spectra for the catalysts under ambient conditions were collected on spinning samples using laser powers of 20–40 mW. The silicalite and titania silicalite samples were calcined at  $500^\circ\text{C}$  for 1–2 h and then cooled to room temperature for  $\frac{1}{2}$  h before taking the Raman spectra. High-temperature *in situ* Raman studies were obtained for stationary samples in a high-purity oxygen (Linde ultrahigh purity) atmosphere flowing through an *in situ* cell made of quartz. Spectral resolution was determined to be approximately  $1\text{ cm}^{-1}$ . Details of the Raman equipment have been described elsewhere.<sup>11</sup>

### Infrared (i.r.) spectroscopy

The amount of Lewis and Brønsted acid sites and the OH vibrations were recorded using an Analect FX-6160 FTi.r. spectrometer. The spectral resolution was determined to be better than  $2\text{ cm}^{-1}$ . The samples were pressed into wafers and pretreated by pulling a vacuum at  $425^\circ\text{C}$  for 1 h *in situ*. The cell was cooled to  $200^\circ\text{C}$  and the spectrum was taken. Pyridine was introduced at 5 Torr and contacted with the samples for 30 s. Desorption of physically adsorbed pyridine was achieved by maintaining the sample in vacuum for 15 min. The concentration of the Lewis and Brønsted acid sites was calculated from the intensities of  $\text{PyH}^+$  and  $\text{PyL}^+$  bands and their extinction coefficients.<sup>12</sup> The margin of error in the measurement of Lewis and Brønsted acid sites observed (individually) was  $\pm 10\text{ }\mu\text{mole/g}$ .

### Catalytic studies

The methanol oxidation reaction was carried out in an isothermal fixed-bed differential reactor maintained at atmospheric pressure and a temperature of  $230^\circ\text{C}$ . The mixture of methanol, oxygen, and helium were in the ratio 7/12/81 (molar %), and total flow

**Table 1** Chemical analysis of the various titania silicalites

Sample nomenclature	Mole% Ti (Ti/Ti + Si)	Weight % of oxide			
		Al	Fe	Na	K
Silicalite #1 TSEx1(0.000)	—	0.07	0.01	0.11	0.01
Ti silicalite #1 TSEx1(0.010)	1.0	0.07	0.08	0.14	0.01
Ti silicalite #1 TSEx1(0.030)	3.0	0.05	0.04	0.11	0.01
Silicalite #2 TSEx2(0.000)	—	0.25	0.05	0.10	0.01
Ti silicalite #2 TSEx2(0.020)	1.3	0.29	0.04	0.06	0.01
Ti silicalite #2 TSEx2(0.200)	1.6	0.28	0.10	0.03	0.01

rates of 25–100 sccm were employed in order to maintain < 5% conversion. The reactor was vertical and made of 6 mm o.d. Pyrex glass. The catalyst was held at the middle of the tube between two layers of quartz wool. The gas flow was from the top to the bottom. Analysis of the product stream was performed using an on-line gas chromatograph (HP 5840) equipped with an FID and two TCDs. The catalytic activities and selectivities are reported only as initial values. Additional details about the experimental arrangement can be found elsewhere.<sup>13</sup>

## RESULTS

### Chemical analysis

The chemical analysis (based on wt% of oxide) of the various TSEx1 and TSEx2 samples is described by Huybrechts et al.<sup>10</sup> and are presented in Table 1. All samples contain varying amounts of Ti and Na, and the TSEx2 samples contain greater amounts of Fe and Al than the TSEx1 samples.

### Raman studies

The Raman spectra of the series of TSEx1 samples are shown in Figure 1. The TSEx1(0.000) sample has Raman bands at 290, 375, 432, 467, 799, 828, 977,

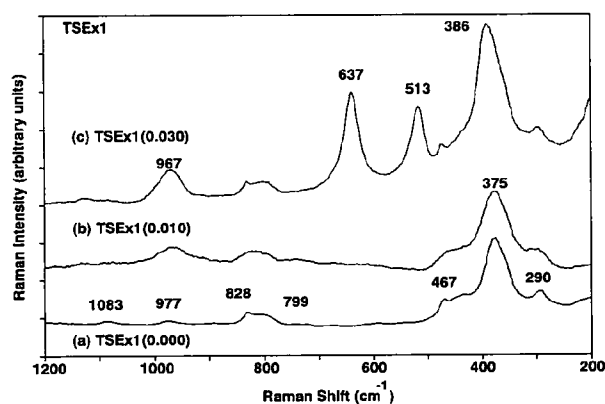


**Figure 1** Ambient Raman spectra of the various Ti silicalites (TSEx1): (a) TSEx1(0.000); (b) TSEx1(0.010); (c) TSEx1(0.030).

and 1083  $\text{cm}^{-1}$ . The major Raman band positions are noted in the figure. The substitution of titania into the TSEx1(0.000) matrix, in TSEx1(0.010), is accompanied by an increase in the relative intensity of the Raman band at  $\sim 970 \text{ cm}^{-1}$ . Further substitution of titania into the TSEx1(0.000) matrix, as in TSEx1(0.030), results in the appearance of Raman bands at 144, 386, 513, and 637  $\text{cm}^{-1}$  that correspond to  $\text{TiO}_2$  (anatase) particles.<sup>14</sup> The Raman band at 144  $\text{cm}^{-1}$  is now shown in the spectrum of TSEx1(0.030) since it is very intense. The band at  $\sim 970 \text{ cm}^{-1}$  is also present with greater intensity relative to the Raman band at 799–828  $\text{cm}^{-1}$ . A detailed analysis of the 1000–1200  $\text{cm}^{-1}$  region of the TSEx1(0.030) sample shows a very weak band at  $\sim 1125 \text{ cm}^{-1}$  developing in the Raman spectra not present in the TSEx1(0.000) spectrum.

The Raman spectra of the series of TSEx2 samples are presented in Figure 2. The Raman spectrum of TSEx2(0.000) exhibits bands at 290, 375, 431, 467, 799, 827, 967, and 1084  $\text{cm}^{-1}$ . As titania is substituted into the silicalite matrix of TSEx2, as in TSEx2(0.020), an increase in the relative intensity of the Raman band at  $\sim 970 \text{ cm}^{-1}$  is observed. Further substitution of the titania into the silicalite matrix of TSEx2, as in TSEx2(0.200), is accompanied by an increase in the relative intensity of the  $\sim 970 \text{ cm}^{-1}$  band and the appearance of a small Raman feature at 143  $\text{cm}^{-1}$  due to a trace of  $\text{TiO}_2$  (anatase) particles. Also present in the titania-substituted TSEx2 samples is a very weak band at  $\sim 1125 \text{ cm}^{-1}$ .

The effect of surface moisture on the titania silicalites was studied by heating the TSEx1(0.010) and TSEx1(0.030) samples to higher temperatures, *in situ*, in an oxygen atmosphere. Figure 3a shows the spectrum of TSEx1(0.030) under ambient conditions and Figure 3b represents the same sample heated to 400°C in oxygen for 0.5 h (the spectrum was obtained after cooling the sample back to room temperature). No change in the spectrum for the TSEx1(0.030) sample is observed in the region above 700  $\text{cm}^{-1}$ . The 100–700  $\text{cm}^{-1}$  region is dominated by the  $\text{TiO}_2$  (anatase) vibrations. Thus, moisture does not appear

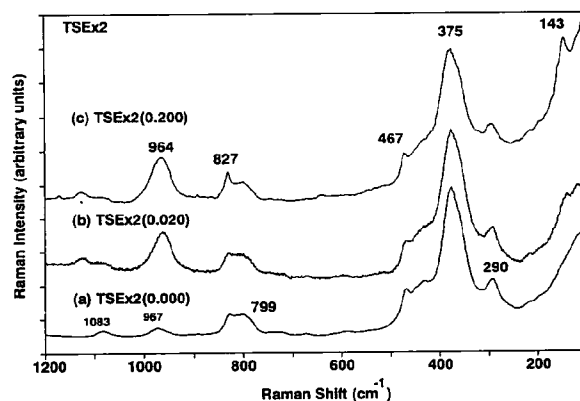


**Figure 2** Raman spectra of the various Ti silicalites (TSEx2): (a) TSEx2(0.000); (b) TSEx2(0.020); (c) TSEx2(0.200).

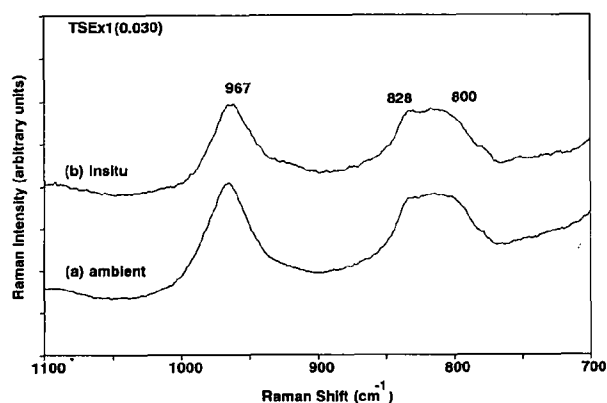


**Figure 3** Raman spectra showing the effect of heat on TSEx1(0.030): (a) obtained under ambient conditions; (b) same sample heated *in situ* to 400°C for 0.5 h and then cooled to room temperature.

to influence the Raman spectrum of titania silicalites. It should be noted that the sample was stationary when the *in situ* Raman spectra were obtained and could have experienced laser-induced dehydration under ambient conditions.

### Effect of calcination temperature

Figure 4 presents the effect of calcination temperature on the TSEx1(0.030) sample. The Raman band at  $\sim 970\text{ cm}^{-1}$ , which is present in all of these samples, does not change with calcination treatment. As described earlier, distinct Raman bands are present at 144, 386, 513, and  $637\text{ cm}^{-1}$ , which are characteristic of  $\text{TiO}_2$  (anatase) particles. On heating the sample up to  $850^\circ\text{C}$ , no change in the bands associated with the  $\text{TiO}_2$  (anatase) particles is observed. The anatase-to-rutile transformation typically occurs at temperatures of  $850^\circ\text{C}$ .<sup>15</sup> Similar observations regarding the structural transformation were also observed with  $\text{TiO}_2$  (anatase) particles dispersed on amorphous  $\text{SiO}_2$  by incipient wetness impregnation.<sup>16</sup>

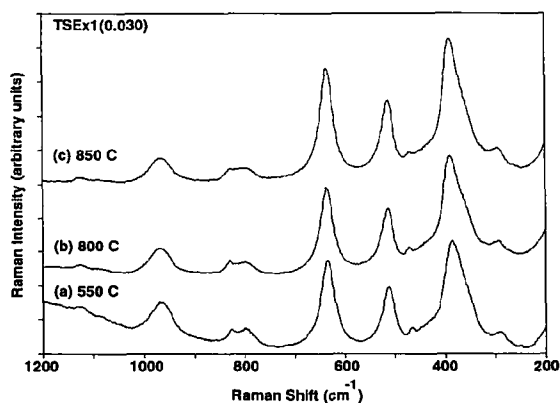


**Figure 4** Raman spectra showing the effect of calcination temperature ( $T$ ) on TSEx1(0.030): (a)  $T = 550^\circ\text{C}$ ; (b)  $T = 800^\circ\text{C}$ ; (c)  $T = 850^\circ\text{C}$ .

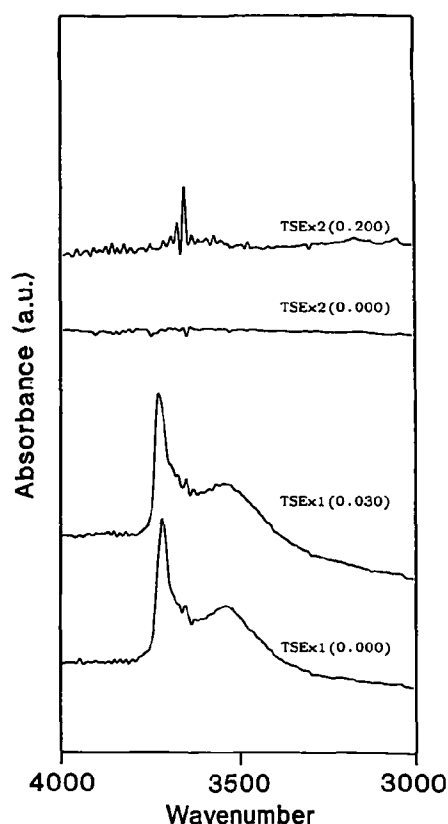


**Figure 5** Infrared spectra showing the hydroxyl region for TSEx1 and TSEx2 samples.

### OH vibrations

Figure 5 contains the i.r. spectra of the OH region as titanium is substituted into the silicalite lattice of TSEx1 and TSEx2 samples. The TSEx2(0.000) sample does not contain any OH vibrations and no OH vibrations are observed upon substituting titania [TSEx2(0.200)]. The TSEx1(0.000) sample, however, has two distinct OH vibrations centred around  $3740$  and  $3540\text{ cm}^{-1}$ , which remain unchanged upon titania substitution. The absence of OH vibrations in the i.r. spectra of the TSEx2(0.000) and TSEx2(0.200) samples and the presence of two OH vibrations in the TSEx1(0.000) and TSEx1(0.030) samples have been independently reported elsewhere.<sup>10</sup>

### X-ray absorption studies

The change of the pre-edge intensity with titania substitution into the silicalite lattice of TSEx1 and TSEx2 samples is shown in Figure 6. The X-ray absorption experiments of the Ti K edge performed under ambient conditions reveal that for the low contents of titania, TSEx1(0.010) and TSEx2(0.020), the normalized pre-edge intensity is  $\sim 0.7$  and  $\sim 0.5$ , respectively, and for the highest loading of titania, TSEx1(0.030), the normalized pre-edge intensity is  $\sim 0.2$ . The titanium pre-edge intensity of the TSEx2(0.200) sample is  $\sim 0.3$ . Analysis

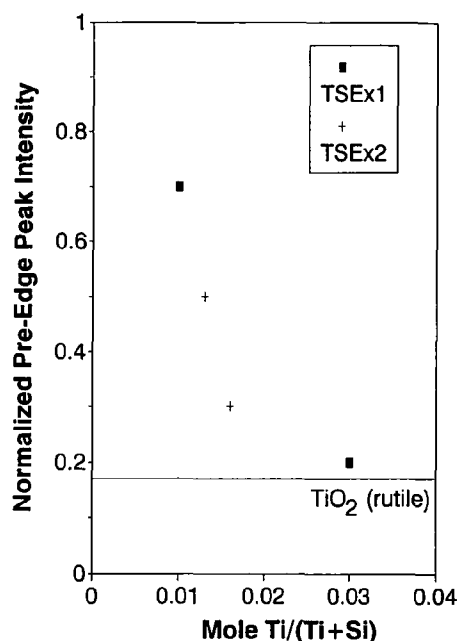


**Figure 6** X-ray absorption pre-edge intensity of the Ti silicalites as a function of titania substitution.

of Figure 6 reveals a decrease in the pre-edge intensity with an increase in titania substitution into the silicalite and the pre-edge intensity approaches values for TiO<sub>2</sub> (rutile) of 0.17 (as shown by the dotted line in Figure 6).<sup>17</sup>

### Pyridine adsorption

The presence of Lewis and Brönsted acid sites in the various samples was probed using pyridine adsorption (see Table 2). Pure SiO<sub>2</sub> and TiO<sub>2</sub> are included for comparison. Pyridine adsorption on the TSEx1(0.000) sample shows only the presence of small amounts of Lewis acid sites. The TSEx1(0.030) sample shows an increase in the Lewis acidity compared to TSEx1(0.000). Pyridine adsorption on the TSEx2(0.000) sample shows the presence of small amounts of Lewis as well as Brönsted acid sites. The TSEx2(0.200) sample shows an increase in Lewis and Brönsted acid sites compared to TSEx2(0.000). The pure SiO<sub>2</sub> (Cab-O-Sil) sample does not exhibit any Brönsted or Lewis acidity. Pure TiO<sub>2</sub> (Degussa) shows only the presence of Lewis acidity.

**Table 2** Lewis (LAS) and Brönsted (BAS) acidity on various Ti silicalites, TiO<sub>2</sub> and SiO<sub>2</sub>

Sample	LAS (μmole/g)	BAS (μmole/g)
1. TSEx1(0.000)	22	0
2. TSEx1(0.030)	50	0
3. TSEx2(0.000)	10	<7
4. TSEx2(0.200)	25	25
5. TiO <sub>2</sub> (P-25, Degussa)	126	0
6. SiO <sub>2</sub> (Cab-O-Sil)	0	0

**Table 3** Methanol oxidation for the various Ti silicalites, TiO<sub>2</sub>, SiO<sub>2</sub>, and 2% TiO<sub>2</sub>/SiO<sub>2</sub> (CH<sub>3</sub>OH = 7/12/81; P = 1 atm; T = 230°C)

Sample	Activity (mole MeOH/gh)	Selectivity (%)
<b>Silicalites (from orthosilicate)</b>		
1. TSEx1(0.000)	No reaction detected under specified conditions	
2. TSEx1(0.010)	$8.0 \times 10^{-3}$	67%, HCHO 18%, CO/CO <sub>2</sub> 15%, HCOOCH <sub>3</sub> trace of CH <sub>3</sub> OCH <sub>3</sub>
3. TSEx1(0.030)	$< 1.0 \times 10^{-4}$	trace of CH <sub>3</sub> OCH <sub>3</sub>
<b>Silicalites (from Ludox)</b>		
4. TSEx2(0.000)	$2.8 \times 10^{-3}$	100%, CH <sub>3</sub> OCH <sub>3</sub>
5. TSEx2(0.200)	$2.9 \times 10^{-2}$	100%, CH <sub>3</sub> OCH <sub>3</sub>
<b>TiO<sub>2</sub> and SiO<sub>2</sub></b>		
6. TiO <sub>2</sub> (P-25, degussa)	$2.3 \times 10^{-3}$	95%, CH <sub>3</sub> OCH <sub>3</sub> 5%, CO/CO <sub>2</sub>
7. SiO <sub>2</sub> (Cab-o-sil)	$1.0 \times 10^{-3}$	100%, CO/CO <sub>2</sub>
8. 2% TiO <sub>2</sub> /SiO <sub>2</sub>	$1.5 \times 10^{-2}$	43%, HCHO 51%, HCOOCH <sub>3</sub> 4%, CO/CO <sub>2</sub> 2%, CH <sub>3</sub> OCH <sub>3</sub>

### Methanol oxidation

The methanol oxidation activities and selectivities of the various TSEx1 and TSEx2 samples are presented in Table 3. The TSEx1(0.000) sample is essentially inactive toward methanol oxidation. Substitution of titania into the silicalite matrix of TSEx1, as in TSEx1(0.020), results in an increase in methanol oxidation activity, and partial oxidation products, HCHO and HCOOCH<sub>3</sub>, are predominantly formed. Further substitution of titania, as in TSEx1(0.030), results in a decrease, by more than an order of magnitude, in methanol oxidation activity, and only traces of dimethyl ether are observed.

The methanol oxidation activity of the TSEx2(0.000) sample, however, is much greater than that of TSEx1(0.000) and dimethyl ether is the only product. Methanol oxidation of titania substituted into the TSEx2(0.000) matrix, as in TSEx2(0.200), shows an increase in methanol oxidation activity and dimethyl ether is again the only reaction product.

For comparison, the methanol oxidation activities and selectivities of TiO<sub>2</sub> particles (P-25, Degussa), amorphous SiO<sub>2</sub> (Cab-O-Sil, Cabot), and 2% TiO<sub>2</sub>/SiO<sub>2</sub> are also presented in Table 2. The TiO<sub>2</sub> particles are slightly active toward methanol oxidation and dimethyl ether is the predominant product. The amorphous SiO<sub>2</sub> sample is weakly active toward methanol oxidation and forms total oxidation products (CO/CO<sub>2</sub>). Adding 2% TiO<sub>2</sub>, as a molecularly dispersed phase, to the amorphous SiO<sub>2</sub> dramatically affects the activity and selectivity for methanol oxidation. The addition of molecularly dispersed titania to amorphous SiO<sub>2</sub> (2% TiO<sub>2</sub>/SiO<sub>2</sub>) results in a more active catalyst and HCHO/HCOOCH<sub>3</sub> are the methanol oxidation products.

## DISCUSSION

Elemental analysis of the various silicalites and titania-substituted silicalites shows that these samples contain silicon, oxygen, titanium, and traces of iron, aluminum, sodium, and potassium. The Raman spectra of the TSEx1 and TSEx2 samples, in the region of interest ( $100\text{--}200\text{ cm}^{-1}$ ), are unaffected by the presence of trace amounts of iron, aluminum, sodium, and potassium because of the low concentrations of these elements as well as their weak Raman signals. Previous studies indicated that titania is present as Ti(IV) in the titania silicalites.<sup>5,8</sup> Therefore, the observed Raman bands of the silicalites and titania-substituted silicalites are associated with the silicon, titanium(IV), and oxygen vibrations.

The TiO<sub>2</sub> (anatase) particles exhibit strong scattering properties and their presence is readily detected by the intense Raman band at  $144\text{ cm}^{-1}$ . The primary observation from the Raman spectra of the various silicalite samples is that the two series of silicalites, TSEx1 and TSEx2, behave similarly toward titania substitution. Furthermore, there are two titania phases present in the Ti silicalites: below 1.60 mole% Ti/(Ti + Si), where TiO<sub>2</sub> particles are not detected (no  $144\text{ cm}^{-1}$  Raman band), titania is present as a dispersed TiO<sub>x</sub> phase; and greater than 1.6 mole% Ti/(Ti + Si), where TiO<sub>2</sub> (anatase) particles ( $144\text{ cm}^{-1}$  Raman band observed) as well as the dispersed TiO<sub>x</sub> phase are present.

The presence of the two different titania phases is confirmed by X-ray absorption spectroscopy studies. The titanium pre-edge intensity for TiO<sub>2</sub> as rutile (octahedral titania) is less than 0.17, and for Ba<sub>2</sub>TiO<sub>4</sub> (tetrahedral titania), 0.84.<sup>17</sup> The drop of the pre-edge intensity from 0.5–0.7 for the TSEx1(0.010) and TSEx2(0.020) samples to  $\sim 0.2$  for the TSEx1(0.030) sample in Figure 6 reflects the presence of TiO<sub>2</sub> particles (octahedral species possessing a center of inversion). This is confirmed by the Raman spectrum of the TSEx2(0.200) sample, which shows distinct features of TiO<sub>2</sub> (anatase) particles. The X-ray absorption spectroscopy studies show that the Ti pre-edge feature, which is related to the average titania coordination, depends upon the amount of titania substituted since essentially two different titania phases are present in the titania silicalites: a dispersed TiO<sub>x</sub> phase and six-coordinated TiO<sub>2</sub> (anatase) particles.

The presence of two titania phases is also consistent with catalytic studies dealing with the epoxidation of 1-octene and oxidation of *n*-hexane where the activity increases linearly with titania substitution (only TiO<sub>x</sub> present) up to  $\sim 1.8$  mole% Ti/(Ti + Si) and then reaches a plateau at higher Ti contents (TiO<sub>x</sub> and TiO<sub>2</sub> particles present).<sup>10</sup> Thus, the combined characterization and reactivity studies indicate that the amount of titania substituted into the silicalites determines the distribution of the two types of titania, and the maximum amount of dispersed titania in the silicalites, using this preparation method, is  $\sim 1.6$  mole% Ti/(Ti + Si). The factors affecting the max-

imum amount of titania that can be substituted in the silicalite are not known at present.

To isolate the vibrations associated with the substituted titania species in the silicalite structure, it is first necessary to assign the vibrations arising from the silicalite matrix. The assignment of the Raman spectra of TSEx1(0.000) and TSEx2(0.000) based on previous literature assignments for silicate materials are the following: the bands at 432, 467, 799–828, and 1083 are assigned to the siloxane linkages (Si–O–Si), and the band at 977, to the silanol group ( $\equiv\text{Si–OH}$ ).<sup>18</sup> The Raman bands at 375 and  $290\text{ cm}^{-1}$  are probably related to the five-, six-, or 10-membered rings present in the silicalite structure.<sup>19</sup> Raman bands associated with three- and four-membered ring vibrations ( $492$  and  $607\text{ cm}^{-1}$ , respectively) appear to be absent from the spectra. Four-membered rings, however, are known to be present in the silicalite structure.

Raman characterization studies on the various Ti silicalites indicate that substitution of the titania into the silicalite lattice results in an increase in the intensity of the Raman band at  $\sim 970\text{ cm}^{-1}$  and the appearance of a new band of low intensity at  $\sim 1125\text{ cm}^{-1}$ . The i.r. studies of the same Ti silicalites also show the presence of a band at  $\sim 960\text{ cm}^{-1}$ , but no i.r. band is observed at  $\sim 1125\text{ cm}^{-1}$ .<sup>10</sup> The integrated intensity of the  $\sim 960\text{ cm}^{-1}$  band in the i.r. increases linearly with the amount of titania substitution until 1.8 mole% Ti/(Ti + Si) and then levels off.<sup>10</sup> An increase in the intensity of the  $\sim 970\text{ cm}^{-1}$  band with titania substitution in Ti silicalites has also been observed previously.<sup>5</sup> The assignment of these additional bands,  $\sim 1125$  and  $\sim 960\text{ cm}^{-1}$ , is crucial to the understanding of the structure of the dispersed TiO<sub>2</sub> species in silicalites since it is directly involved in the mild oxidation reactions using hydrogen peroxide.<sup>10</sup> The possible vibrations that might give rise to the  $\sim 970\text{ cm}^{-1}$  band are the silanol ( $\equiv\text{Si–OH}$ ) vibration, the SiO<sup>δ-</sup>–Ti<sup>δ+</sup> vibration,<sup>6</sup> or the Ti=O vibration originally proposed.<sup>5</sup> It is necessary to discriminate among these different possibilities to arrive at a possible structural characterization of the TiO<sub>x</sub> species.

The Raman spectra of the silicalites, TSEx1(0.000) and TSEx2(0.000), exhibit a weak band at  $967\text{--}977\text{ cm}^{-1}$ . A similar band at  $978\text{ cm}^{-1}$  is observed in the Raman spectra of amorphous SiO<sub>2</sub> (Cab–O–Sil) arising from the silanol ( $\equiv\text{Si–OH}$ ) vibrations. This silanol vibration intensity is closely related to the  $3748\text{ cm}^{-1}$  OH vibration intensity<sup>18</sup> and an increase in intensity of the  $978\text{ cm}^{-1}$   $\equiv\text{Si–OH}$  vibration of amorphous SiO<sub>2</sub> should have a corresponding increase in intensity of the  $3748\text{ cm}^{-1}$  OH vibration. One possibility is that upon substituting titania into the silicalite matrix more silanol groups are produced due to structural rearrangements. For TSEx1(0.000), the presence of OH vibrations are evident at  $3748\text{ cm}^{-1}$  (Figure 5). A broad band is also present at  $3540\text{ cm}^{-1}$  in the OH region for TSEx1(0.000) and is assigned to interacting OH groups.<sup>10</sup> The presence of OH groups, however, are not detected in the i.r. spectra of

TSEx2(0.000), but small amounts are observed in the cross-polarization  $^1\text{H}$ - $^{29}\text{Si}$  n.m.r. studies.<sup>10</sup> The substitution of titania into the silicalite matrix results in an increase in intensity of the  $970\text{ cm}^{-1}$  band in the Raman spectra (Figures 1 and 2), but no corresponding increase is observed in the OH region (Figure 5). Thus, the increase in intensity of the  $\sim 970\text{ cm}^{-1}$  band in the titania-substituted silicalite samples is not due to the creation of additional  $\equiv\text{Si-OH}$  groups. However, the  $967\text{--}977\text{ cm}^{-1}$  band originally present in the silicalites, TSEx1(0.000) and TSEx2(0.000), is due to the  $\equiv\text{Si-OH}$  vibrations. Furthermore, recent experiments have shown the  $950\text{--}975\text{ cm}^{-1}$  band of Ti silicalites is not affected by deuterium exchange and, thus, is not associated with the  $\equiv\text{Si-OH}$  vibration.<sup>20</sup>

A systematic Raman study of various titanate compounds reveals that the highest titanium-oxygen vibrational mode occurs at  $900\text{ cm}^{-1}$ .<sup>16</sup> Four-coordinated ( $\text{TiO}_4$ ) compounds possess their highest vibrations between  $700$  and  $800\text{ cm}^{-1}$ , a five-coordinated ( $\text{TiO}_5$ ) compound exhibits its highest vibration at  $900\text{ cm}^{-1}$ , and six-coordinated ( $\text{TiO}_6$ ) compounds possess their highest vibration between  $600$  and  $800\text{ cm}^{-1}$  depending on the extent of distortion of the  $\text{TiO}_6$  unit. Only in acidic aqueous solutions is there a Raman band at  $\sim 960\text{ cm}^{-1}$  due to hydrous titanyl species,  $\text{Ti=O}^{2+}$ ,<sup>21,22</sup> but this titania species is not present in any solid titanate compounds studied. X-ray absorption studies on TS-2 materials show the absence of any  $\text{Ti=O}$  bonds even though the  $960\text{ cm}^{-1}$  i.r. band is still present.<sup>23</sup> Thus, the Ti silicalite Raman bands at  $\sim 970$  and  $1115\text{ cm}^{-1}$  cannot be related to  $\text{Ti-O}$  vibrational modes since all solid titania compounds possess Raman bands below  $900\text{ cm}^{-1}$ . Furthermore, the vibrational modes at  $\sim 970$  and  $\sim 1115\text{ cm}^{-1}$  are also observed in the Raman spectra for vanadium silicalite,<sup>24</sup> and silicate glasses<sup>25</sup> and suggests that they are related to silica vibrations rather than the incorporated cations (Ti, V, K, Na, Ca, etc.).

A detailed review of silicate Raman vibrations shows that vibrations arise in the  $950\text{--}960$  and  $1110\text{--}1120\text{ cm}^{-1}$  region when cations are introduced into silicate materials.<sup>25</sup> In the high-frequency region ( $800\text{--}1200\text{ cm}^{-1}$ ), Raman bands are assigned to the symmetric silicon-oxygen stretching motions of silicate units with one, two, three, and four nonbridging oxygens. These bands give rise to polarized Raman bands at  $1100\text{--}1050$ ,  $1000\text{--}950$ ,  $\sim 900$ , and  $\sim 850\text{ cm}^{-1}$ , respectively, and weak depolarized Raman bands at  $1200$  and  $1060\text{ cm}^{-1}$  due to asymmetric silicon-oxygen vibrations within a fully polymerized tetrahedral network. Based on these observations, the  $1115\text{ cm}^{-1}$  band in the Ti silicalites can be assigned to the  $\text{SiO}_4$  unit containing a single nonbridging oxygen (denoted as  $\equiv\text{SiO}$  in Ref. 25 and the  $950\text{--}960\text{ cm}^{-1}$  band can be assigned to the vibration of two nonbridging oxygens (denoted as  $=\text{SiO}_2$  in Ref. 25). Thus, vibrational spectroscopies (Raman and i.r.) do not provide direct structural information regarding the titania species in the Ti silicalites since the vibra-

tions observed are essentially those arising due to silicon-oxygen vibrations. However, the vibrational spectroscopies give direct information on the state of the dispersed titania cations incorporated into the silicalite matrix that give rise to the  $\sim 960\text{ cm}^{-1}$  band in i.r. and Raman or present as a separate crystalline phase (bands at  $\sim 637$ ,  $513$ ,  $386$ , and  $144$  for  $\text{TiO}_2$  [anatase]).

To obtain structural information about the titania species in the Ti silicalites, it is necessary to undertake detailed experiments with other structural spectroscopic techniques such as X-ray absorption spectroscopy that can provide direct structural information about the Ti sites. The continuous decrease in the Ti K pre-edge intensity as a function of titania substitution as shown in Figure 6 suggests that the (average) structure of the dispersed  $\text{TiO}_x$  species is constantly changing with titania substitution even prior to  $\text{TiO}_2$  (anatase) particle formation. The high pre-edge intensity of the TSEx1(0.010) and TSEx2(0.020) samples indicates that the major fraction of the  $\text{TiO}_x$  species in these samples does not possess a center of inversion (presumably tetrahedral). The presence of only trace amounts of  $\text{TiO}_2$  (anatase) particles that are observed in the Raman spectra of the TSEx2(0.200) sample cannot account for the drop of the pre-edge intensity to  $\sim 0.3$ .

This suggests that the (average) structure of the dispersed  $\text{TiO}_x$  species in the TSEx2(0.200) sample is different from that in the TSEx1(0.010) and TSEx2(0.020) samples and the major fraction of the  $\text{TiO}_x$  species in the TSEx2(0.200) sample possesses a center of inversion (presumably octahedrally coordinated). The continuous decrease in pre-edge intensity with titania substitution is similar to the results obtained on TS-2 samples by Trong On et al.<sup>23</sup> For the TS-2 samples, the decrease in the pre-edge intensity was related to the change in distribution of tetrahedral, square pyramidal, and octahedral  $\text{TiO}_x$  species. The titania silicalite samples (TS-1) in the present study appear to behave similarly to the TS-2 samples. Correlating the present structural information with the reactivity of the titania silicalites involving liquid water suggests that the (average) structure of the  $\text{TiO}_x$  phase does not apparently affect the reactivity of the active site since the catalytic activity increases linearly with increase in titania substitution in the silicalites in this region.<sup>10</sup>

Under ambient conditions, oxide surfaces usually possess surface moisture that coordinates with the active sites. This surface moisture desorbs at high temperatures, which is usually the case under most reaction conditions. Consequently, characterization of the active site of catalytic materials under ambient conditions is only possible if moisture is not present.<sup>26</sup> It can be observed from Figure 3 that heating the samples to higher temperatures does not influence the Raman band at  $\sim 970\text{ cm}^{-1}$  and, thus, this band arises from a dehydrated species. This observation of dehydrated species is not surprising since silicalites are hydrophobic by nature<sup>19</sup> and are expected to lose moisture readily especially when mildly heated by the

laser light. However, i.r. and X-ray absorption studies involving adsorption of moisture indicates that moisture has an effect on the  $\sim 970\text{ cm}^{-1}$  band.<sup>6,9</sup> Most likely, the dehydration of the titania silicalite occurs in the laser beam and the  $\sim 970\text{ cm}^{-1}$  is, indeed, due to the dehydrated Ti silicalite.

Acidity measurements using pyridine adsorption show that all of the TSEx1 and TSEx2 samples possess weak Lewis acidity per gram of sample compared to bulk  $\text{TiO}_2$ . The slight increase in Lewis acidity for TSEx1(0.030) is attributed to the presence of  $\text{TiO}_2$  (anatase) particles, which is observed in the Raman spectrum. Aluminum and iron oxides present in zeolites give rise to Brønsted acidity,<sup>27</sup> and the presence and increase of Brønsted acidity in the TSEx2(0.000) and TSEx2(0.200) samples follows this trend. The amount of Lewis acid sites for the TSEx2(0.000) and TSEx2(0.200) sites are similar.

Methanol oxidation is a useful chemical probe for distinguishing between surface acid and redox sites.<sup>13</sup> TSEx1(0.000) is inactive toward methanol oxidation, indicating weak or no acid or redox sites. Redox activity is observed as titania is substituted into the TSEx1(0.000) matrix to form  $\text{TiO}_x$  species. This suggests that the  $\text{TiO}_x$  species act as a redox site in the presence of molecular oxygen. Redox sites are also present for the 2%  $\text{TiO}_2/\text{SiO}_2$ , which contains molecularly dispersed titania on an amorphous  $\text{SiO}_2$  support. Bulk  $\text{TiO}_2$ , on the other hand, is an order of magnitude less active than the 2%  $\text{TiO}_2/\text{SiO}_2$  sample and only yields dimethyl ether due to the presence of Lewis acid sites on the surface. Further addition of titania into the silicalite matrix [TSEx1(0.030)], which results in the formation of  $\text{TiO}_2$  (anatase) particles, results in a drop in activity and the formation of dimethyl ether. The complete absence of any detectable redox products for the TSEx1(0.030) sample indicates either (1) formation of  $\text{TiO}_2$  (anatase) particles as the predominate titania phase or (2) pore blockage due to the  $\text{TiO}_2$  (anatase) particles that make the  $\text{TiO}_x$  species inaccessible. The similar reactivity and selectivity of the Ti silicalite and 2%  $\text{TiO}_2/\text{SiO}_2$  catalysts toward methanol oxidation suggests that the Si ligand is controlling the reactivity of the Ti sites. Thus, incorporating Ti into the crystalline silicalite lattice cannot alter the intrinsic reactivity of the Ti sites coordinated to Si since Si is the ligand in both the amorphous (2%  $\text{TiO}_2/\text{SiO}_2$ ) and the crystalline (Ti silicalite) systems.

The high activity of TSEx2(0.000) for dimethyl ether is due to the presence of aluminum and iron oxide impurities that give rise to acid sites (see Table 2) and overshadows any redox activity of the titania species. The activity of TSEx2(0.200) is one order of magnitude greater than that of TSEx2(0.000), which is related to the higher amounts of aluminum and iron oxide impurities present. The presence of acid sites in the TSEx2(0.200) sample produces dimethyl ether during methanol oxidation and is also responsible for the acid side reactions in the hydroxylation of phenol.<sup>10</sup>

It is also relevant to compare the crystalline Ti

silicalite system with the amorphous surface titania-supported silica system. The surface titania on amorphous silica catalysts has recently been characterized by Raman, high-resolution TEM, and XANES.<sup>28-30</sup> Under ambient conditions, where the surface is hydrated, XANES measurements reveal that the surface titania phase on amorphous silica does not possess a center of inversion<sup>30</sup> and Raman measurements reveal the presence of a broad band at  $940\text{--}960\text{ cm}^{-1}$ .<sup>28</sup> These characteristic bands are representative of  $\text{Ti}=\text{O}^{+2}$  species typically present in acidic aqueous solutions. The low isoelectric point of the silica surface,  $2 < \text{pH} < 4$ , maintains the thin aqueous film at a low pH value.<sup>31</sup> Under *in situ* dehydrated conditions, the broad Raman band at  $950\text{--}960\text{ cm}^{-1}$  is not present for the surface titania phase on amorphous silica.<sup>29</sup> The absence of this band under dehydrated conditions demonstrates that the  $\text{Ti}=\text{O}^{+2}$  species is not present under *in situ* conditions, but new Raman features are not observed for the  $\text{TiO}_2/\text{SiO}_2$  sample because of the weak titania signal and the strong background from the amorphous silica support at other frequencies. More recent *in situ* dehydration investigations of a 10%  $\text{TiO}_2/\text{SiO}_2$  sample indicates the presence of Raman bands at 910 and  $1180\text{ cm}^{-1}$ .<sup>32</sup> Analogous to Raman vibrations of silicate materials, these bands are tentatively assigned to Si-O vibrations and do not provide additional structural information about the surface titania species.<sup>25</sup> Corresponding *in situ* XANES measurements for the surface titania on amorphous silica have not been performed. The change in the Raman features of the surface titania phase supported on amorphous silica with hydration/dehydration confirms that it is indeed a surface phase,<sup>26</sup> and such surface phases are known to break their M-O-Si bond via hydrolysis when exposed to moisture.<sup>33</sup> The presence of moisture, however, only has a mild influence on Ti silicalite since the  $960\text{--}970\text{ cm}^{-1}$  band exhibits only a slight shift and broadening in the presence of moisture.<sup>6</sup> Thus, it appears that the Ti-O-Si bonds present in the crystalline Ti silicalite are not easily hydrolyzed, whereas the Ti-O-Si bonds present on the surface of amorphous silica can be readily hydrolyzed.

The different stabilities of the Ti-O-Si bonds for Ti silicalite and surface titania on amorphous silica in the presence of moisture appears to account for the catalytic properties of these titania-silica materials. The methanol oxidation reaction is conducted at elevated temperatures and at very low partial pressures of water (low conversion of methanol), and under these conditions, the Ti-O-Si bonds are not hydrated in the crystalline Ti silicalites or the titania dispersed on amorphous silica. Consequently, the catalytic properties of Ti silicalite and surface titania on amorphous silica are very similar since the Ti-O-Si bond is involved in this reaction.<sup>34</sup> A very different situation results when the oxidation reaction occurs at milder temperatures and in the presence of liquid water.<sup>1,10</sup> The surface titania on amorphous silica catalyst cannot function under these conditions because the Ti-O-Si bond is hydrolyzed and the titania



component is not bound to the silica surface. However, the titania component in Ti silicalite is not hydrolyzed under these conditions because it is part of the crystalline silicalite lattice and, consequently, can continue to function in the presence of liquid water. The hydrophobic nature of the silicalite matrix probably also minimizes the amount of water present in the pores. The participation of the Ti–O–Si bond of the titania silicalites in reactions involving liquid water may be the reason why reactivity of titania silicalites is independent of the TiO<sub>x</sub> structure and just depends on the formation of the Ti–O–Si bond. Thus, the stability of the Ti–O–Si bond in the presence of water appears to be a critical factor in determining the reactivities of Ti silicalites and surface titania supported on amorphous silica.

## CONCLUSIONS

Upon substitution of titania into the silicalite matrix, the titania species is present as TiO<sub>x</sub> species or TiO<sub>2</sub> (anatase) particles in the Ti silicalites. The relative amount of TiO<sub>x</sub> and TiO<sub>2</sub> (anatase) particles depends on the amount of titanium substituted into the silicalite matrix. Below 1.6 mole% Ti/(Ti + Si), titania is present as a dispersed TiO<sub>x</sub> species. The TiO<sub>2</sub> (anatase) particles are formed above 1.6 mole% Ti/(Ti + Si) in addition to the TiO<sub>x</sub> species. The TiO<sub>x</sub> species (1) does not possess a terminal Ti=O bond; (2) changes structure with titania substitution into the silicalite matrix, but (3) the structural change does not, apparently, change the reactivity of the catalytic active site in reactions involving liquid water; (4) is a redox site that is able to undergo oxidation reaction by molecular oxygen; and (5) does not possess Brønsted acidity. The TiO<sub>2</sub> (anatase) particles are stable even after high-temperature calcination and form weak Lewis acid centers. The difference in the chemical behavior of the two silicalites synthesized from the two different silica precursors is due to the aluminum and iron oxide impurities, which are responsible for the formation of acid sites and, consequently, give rise to acid side reactions. The critical factor in determining the reactivities of Ti silicalite and surface titania supported on amorphous silica is the stability of the Ti–O–Si bond in the presence of water.

## ACKNOWLEDGEMENTS

The authors wish to thank Dr. F.D. Hardcastle for critically reviewing the manuscript and providing constructive comments. G.D. and I.E.W. would like to thank the National Science Foundation for their financial support (NSF Grant # CTS 9006258).

## REFERENCES

- US Patent 4 410 501 (1983) (to Snamprogetti).
- Huybrechts, D.R.C., Bruycker, L.De and Jacobs, P.A., *Nature* 1990, **345**, 240
- Huybrechts, D.R., Vaesen, I., Li, H.X. and Jacobs, P.A. *Catal. Lett.* 1991, **8**, 237
- Clerici, M. *Appl. Catal.* 1991, **249**, 68
- Perego, G., Bellussi, G., Corno, C., Taramasso, M., Buonomo, F. and Esposito, A., in *New Developments in Zeolite Science and Technology, Proceedings of the 7th International Zeolite Conference, Tokyo*, August 17–22, 1986 (Eds. Y. Murakami, A. Iiiuma and J.W. Ward) Kodansha/Elsevier, Tokyo/Amsterdam, 1986, p.129
- Boccuti, M.R., Rao, K.M., Zecchina, A., Leofanti, G. and Petrini, G., *Stud. Surf. Sci. Catal.* 1989, **48**, 133
- Ashton, A.G., Dwyer, J., Elliott, I.S., Fitch, F.R., Oin, G., Greenwood, M. and Speakman, J., in *Proceedings of the Sixth International Conference on Zeolites, Reno* (Eds. D. Olson and A. Bisio) Butterworth, Guildford, UK, 1984, p.704
- Tuel, A., Diab, J., Gelin, P., Dufaux, M., Dutel, J.-F. and Taarit, Y.B. *J. Mol. Catal.* 1990, **63**, 95
- (a) Behrens, P., Felsche, J. and Niemann, W. *Catal. Today* 1991, **8**, 479. (b) Behrens, P., Felsche, J., Vetter, S., Schulz-Ekloff, G., Jaeger, N.I. and Niemann, W. *J. Chem. Soc., Chem. Commun.* 1991, 678
- Huybrechts, D.R.C., Buskens, Ph. and Jacobs, P.A. *J. Mol. Catal.* 1992, **71**, 129
- Wachs, I.E., Hardcastle, F.D. and Chan, S.S. *Spectroscopy* 1986, **1**, 30
- Turek, A.M. Datka, J. and Wachs, I.E. *J. Catal.* 1992, **96**, 5000
- Deo, G., Eckert, H. and Wachs, I.E. *ACS Petrol. Chem. Div. Prepr.* 1990, **35**(1), 16
- Wachs, I.E. and Hardcastle, F.D., in *Proceedings of the 9th International Congress on Catalysis*, 1988, Vol. 3, p.1449
- Shannon, R.D. *J. Appl. Phys.* 1964, **34**, 3414
- (a) Hardcastle, F.D. and Peden, C.H., in *201st ACS National Meeting, Atlanta, Georgia, April 1991*, paper 84. (b) Hardcastle, F.D. and Peden, C.H., submitted
- Greeger, R.B., Lytle, F.W., Sandstorm, D.R., Wong, J. and Schultz, P. *J. Non-Cryst. Solids* 1983, **55**, 27
- (a) Tallant, D.R., Bunker, B.C., Brinker, C.J. and Balfe, C.A. *Mat. Res. Soc. Symp. Proc.* 1986, **73**, 261. (b) Stolen, R.H. and Walrafen, G.E. *J. Chem. Phys.* 1976, **64**(6), 2623. (c) Brinker, C.J., Tallant, D.R., Roth, E.P. and Ashley, C.S. *Mat. Res. Soc. Symp. Proc.* 1986, **61**, 387
- Fyfe, C.A., Gobbi, G.C., Klinowski, J., Thomas, J.M. and Ramdas, S. *Nature* 1982, **296**, 530
- Bellussi, G., Carati, A., Clerici, M.G., Maddinelli, G. and Millini, R. *J. Catal.* 1992, **133**, 220
- Reichmann, M.G. and Bell, A.T. *Langmuir*, 1987, **3**, 111
- (a) Gratzel, M. and Rotzinger, F.P. *Inorg. Chem.* 1985, **24**, 2321. (b) Comba, P. and Merbach, A. *Inorg. Chem.* 1987, **26**, 1315
- Trong On D., Bonneviot, L., Bittar, A., Sayari, A. and Kaliaguine, S. *J. Mol. Catal.* 1992, **74**, 233
- Turek, A.M., Arora, N., Deo, G., Wachs, I.E., Rigutto, M.S. and van Bekkum, H., unpublished work
- P. Mcmillan, *Am. Miner.* 1986, **69**, 622
- Chan, S.S., Wachs, I.E., Murrell, L.L., Wang, L. and Hall, W.K. *J. Phys. Chem.* 1984, **88**, 5831
- Connell, G. and Dumesic, J.A. *J. Catal.* 1986, **102**, 216
- Srinivasan, S., Datye, A., Hampden-Smith, M., Wachs, I.E., Deo, G., Jehng, J.M., Turek, A.M. and Peden, C.H.F. *J. Catal.* 1991, **131**, 260
- Jehng, J.-M. and Wachs, I.E. *Catal. Lett.* 1992, **13**, 9
- Wong, J. and Wachs, I.E., presented at the Materials Research Society Meeting, Boston, MA, Nov. 28–Dec. 2, 1988, paper D32
- Deo, G. and Wachs, I.E. *J. Phys. Chem.* 1991, **89**, 5889
- Hu, H. and Wachs, I.E., unpublished work
- de Boer, M., van Dillen, A.J., Koningsberger, D.C., Geus, J.W., Vuurman, M.A. and Wachs, I.E. *Catal. Lett.* 1991, **11**, 227
- Deo, G. and Wachs, I.E. *J. Catal.* 1991, **129**, 137